Sequence-Dependent Assembly

DOI: 10.1002/anie.201207467

Sequence-Dependent Assembly to Control Molecular Interface Properties**

*Graham de Ruiter, Michal Lahav, Hodaya Keisar, and Milko E. van der Boom**

Functional molecular materials have been obtained by liquid/vapor-phase epitaxy or layer-by-layer (LbL) assembly with 1) electro-optic responses sufficiently high to build high-speed electro-optical modulators,[1] 2) high-*k* dielectrics for fabricating organic field effect transistors (OFETs),[2] and 3) ultra-low-β materials to generate molecular wires.[3] Moreover, combining metal–ligand coordination chemistry with stepwise solution-based deposition resulted in the formation of crystalline assemblies, including highly porous metal–organic frameworks (MOFs) on inorganic surfaces.[4] The key for fabricating these and other molecular materials is frequently found in a highly conserved assembly sequence that directs them towards their unique properties and desired function. Similarly, nature dictates the function of enzymes and the genetic information encoded in DNA/RNA by means of the sequence in which the amino acids and nucleotides are arranged. Yet nature is able to create diverse functionalities with the same molecular building blocks. An intriguing question thus remains; can we harvest new and useful material properties by only changing the assembly sequence of the molecular components?

To address this challenge, we introduce herein a sequence-dependent assembly (SDA) of molecular interfaces and show how this strategy—specific to a set of given building blocks—can be fully exploited to form self-propagating molecule-based assemblies (SPMAs) with diverse functionalities. Each SPMA (I–IV) was formed with the same molecular complexes (**1**, **2**) that subdivides our sequence-dependent assembly into four branches: (I) alternating assembly of **1** and **2**; (II) successive assembly of molecular component **1**, then complex **2**; (III) successive assembly of molecular component **2**, then **1**; and (IV) assembly of the molecular components from a mixture of **1** and **2** (Scheme 1).[5] The difference between each branch of the sequence-dependent assembly is

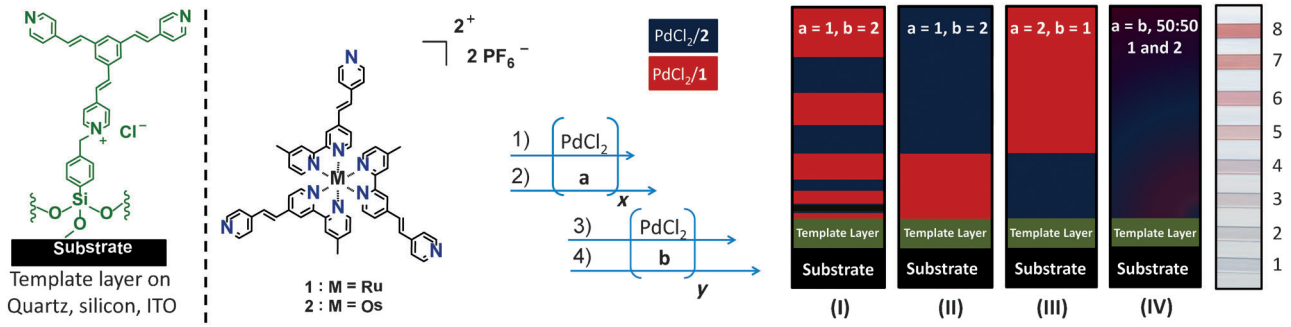

Scheme 1. Sequence-dependent assembly method of preparing self-propagating molecule-based assemblies I-IV. The interfaces are formed by immersion of a pyridine-terminated template layer on quartz, silicon and ITO-coated glass substrates[10] in a 1.0 mM THF solution of $[Pd(PhCN)_2Cl_2]$ and subsequent immersion in 0.2 mM solutions of complexes **1** or **2** in THF/DMF (9:1 v/v) followed by immersion . The different self-propagating molecule-based assemblies were created by alternate repetition of steps *x* and *y* (I and IV) or successive repetition of steps *x* and *y* (II and III). The photograph on the right shows the coloration of the self-propagating molecule-based assembly-functionalized ITO-coated glass substrates (7.5 cm × 0.8 cm) as a function of the number of deposition steps.

undoubtedly reflected in the multi-faceted electrochemical properties of the corresponding self-propagating molecule-based assemblies. Furthermore, for sequence-dependent assembly II and III, we can control the pathway by which electron transfer occurs by tuning the surface–interface thickness of the molecular components (**1**, **2**). The delicate interplay between the sequence-dependent assembly and the surface–interface thickness resulted in four distinctly observable electrochemical signatures: 1) reversible electron transfer, 2) oxidative catalytic electron transfer with charge trapping, 3) reductive catalytic electron transfer, and 4) blocking of the electron transfer. The importance of the appropriate sequence-dependent assembly strategy is not only paramount

[*] G. de Ruiter, Dr. M. Lahav, H. Keisar, Prof. M. E. van der Boom
Department of Organic Chemistry, Weizmann Institute of Science
76100 Rehovot (Israel)
E-mail: milko.vanderboom@weizmann.ac.il
Homepage: https://sites.google.com/site/milkovanderboomslab/

[**] This research was supported by the Helen and Martin Kimmel Center for Molecular Design, Mary and Tom Beck-Canadian Center for Alternative Energy Research, David Rosenberg (Chicago, IL), the Yeda-Sela Center for Basic Research, a research grant from the Leona M. and Harry B. Helmsley Charitable Trust, and the Israel Science Foundation (ISF) Grant No. 289/09. M.B. is the incumbent of the Bruce A. Pearlman Professorial Chair in Synthetic Organic Chemistry.

Supporting information for this article is available on the WWW under http://dx.doi.org/10.1002/anie.201207467.

in forming surface-confined molecular interfaces; it might also be applied in self-sorting assemblies, molecular networking, and multi-component MOFs, in which instances of sequential order can be identified.[6]

For construction of the self-propagating molecule-based assemblies by our sequence-dependent assembly strategy we relied on our recent examples of molecule-based materials that are active participants in their continuing self-propagating assembly.[7] These materials have already been applied in electrochromic materials, solar cells, and molecular data storage.[8] The exponential growth processes observed in these assemblies involves absorption of an excess of a palladium salt into a unimolecular network consisting of complex **2** linked by palladium dichloride.[9] For our self-propagating molecule-based assemblies (SPMAs I–IV; numbers coincide with the sequence-dependent assembly strategy I–IV employed in their preparation), composed of complexes **1** and **2**, similar growth processes and identical optical properties have been observed (Supporting Information, Figure S1).

In sequence-dependent assembly I, the molecular components (**1**, **2**) are arranged in an alternating manner to give a self-propagating molecule-based assembly that is 11.4 nm thick (SPMA I | Ru_2-Os_2). The cyclic voltammogram (CV) of this self-propagating molecule-based assembly exhibits reversible electrochemical waves for both the $Os^{2+/3+}$ and $Ru^{2+/3+}$ redox couples (Figure 1 A). Furthermore, the electrochemical behavior is reversible and surface-confined up to a thickness of 54 nm, although a decrease in the electron transport kinetics was observed (Figure S2 and S3). The Os/Ru ratio does not vary significantly during self-propagating molecule-based assembly growth as shown by a similar total charge for both redox processes (Ru: $Q = 0.92 \times 10^{-4}$ C and Os: $Q = 1.13 \times 10^{-4}$ C: Figure S4).

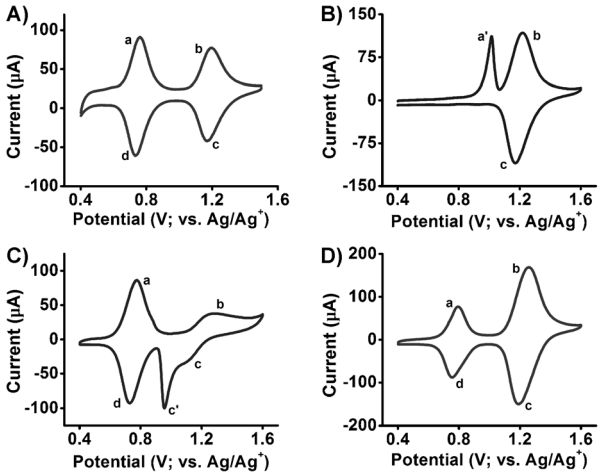

Figure 1. Cyclic Voltammograms (CVs) of self-propagating molecule-based assemblies constructed by sequence-dependent assembly (Scheme 1). The CVs of SPMAs, on ITO, were recorded at a scan rate of 200 $mV s^{-1}$, with thicknesses of A) 11.4 nm (SPMA I | Ru_2-Os_2); B) 12.1 nm (SPMA II | Ru_3-Os_1); C) 11.4 nm (SPMA III | Os_3-Ru_2); and D) 12.5 nm (SPMA IV | $(Ru\text{-}Os)_4$). The oxidation/reduction processes in the SPMAs are indicated by the lettered potentials and are defined as follows: $Os^{2+} \rightarrow Os^{3+}$ (a); catalytic $Os^{2+} \rightarrow Os^{3+}$ (a'); $Ru^{2+} \rightarrow Ru^{3+}$ (b); $Ru^{3+} \rightarrow Ru^{2+}$ (c); catalytic $Ru^{3+} \rightarrow Ru^{2+}$ (c'); and $Os^{3+} \rightarrow Os^{2+}$ (d).

The half-wave potentials for **1** and **2** in SPMA I | Ru_2-Os_2 are similar to the ones measured in solution (**2**: 0.758 V and **1**: 1.180 V (SPMA) vs. **2**: 0.770 V and **1**: 1.200 V (solution; Figure S5) and the large separation of the half-wave potentials of $\Delta E_{1/2} = 422$ mV ($\Delta E_{1/2} = \Delta E_{1/2}Ru - \Delta E_{1/2}Os$), indicates that no communication exists between the different metal-centers on the surface (Figure 1 A). This is an important characteristic that allows both types of metal-centers to be addressed individually. This feature is only displayed in products obtained by sequence-dependent assembly strategies I and IV, whereas for the products sequence-dependent assembly II and III metal–metal communication is observed (Figure 1 B and C, see below).

In sequence-dependent assembly II, complexes **1** and **2** are deposited successively, the electrochemical properties are markedly affected, by the presence of the inner ruthenium layer. For a self-propagating molecule-based assembly with a Ru thickness of 8.0 nm and an Os thickness of 4.1 nm (SPMA II | Ru_3-Os_1), the electrochemical behavior exhibits a sharp catalytic oxidative pre-wave at approximately 1.08 V (Figure 1 B and 2 A; red trace). Furthermore, the intensity of

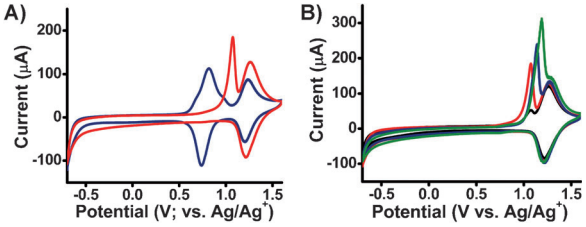

Figure 2. CVs of self-propagating molecule-based assemblies constructed by sequence-dependent assembly (Scheme 1). A) CV of SPMAs on ITO at 200 $mV s^{-1}$ with a Ru thickness of 5.7 nm and an Os thickness of 6.8 nm (SPMA II | Ru_2-Os_2; blue trace) and with a Ru thickness of 8.0 nm and an Os thickness of 4.1 nm (SPMA II | Ru_3-Os_1; red trace) showing the generation of the oxidative pre-wave at approximately 1.08 V upon increasing the Ru thickness. B) CV of SPMAs on ITO at 200 $mV s^{-1}$ with increasing thicknesses of the Os layer from 4.1 nm (red trace; SPMA II | Ru_3-Os_1) to 9.3 nm (blue trace; SPMA II | Ru_3-Os_2), and finally to 17.6 nm (green trace; SPMA II | Ru_3-Os_3). The black trace shows the CV of an SPMA with only Ru (SPMA II | Ru_3-Os_0).

this catalytic pre-wave increased significantly upon increasing the surface–interface thickness of the osmium layer from 4.1 nm (Figure 2 B; red trace SPMA II | Ru_3-Os_1), to 9.3 nm (Figure 2 B; blue trace—SPMA II | Ru_3-Os_2) and finally to 17.6 nm (Figure 2 B; green trace—SPMA II | Ru_3-Os_3). Thus this sharp pre-wave at approximately 1.08 V results from catalytic oxidation of the Os metal centers in the outer layer of SPMA II | Ru_3-Os_1.[11] This effect can be explained—similar to Murray's explanation[11]—by assuming that the inner Ru layer (8.0 nm) isolates the Os metal centers from the ITO electrode. Therefore, at the half-wave potential of the $Os^{2+/3+}$ redox couple no oxidation/reduction is observed. However, at the onset potential for Ru oxidation, oxidation starts to occur from $Ru^{2+} \rightarrow Ru^{3+}$. Since the thermodynamic parameters are such that Ru^{3+} is able to oxidize Os^{2+}, and Ru^{3+} is constantly regenerated through self-exchange with the ITO electrode, a conductive path is formed from the ITO electrode. There-

fore, the sparingly formed Ru^{3+} centers, behave as a catalytic gate for electron transport from osmium to the ITO electrode. This process is graphically illustrated in Scheme 2 A.

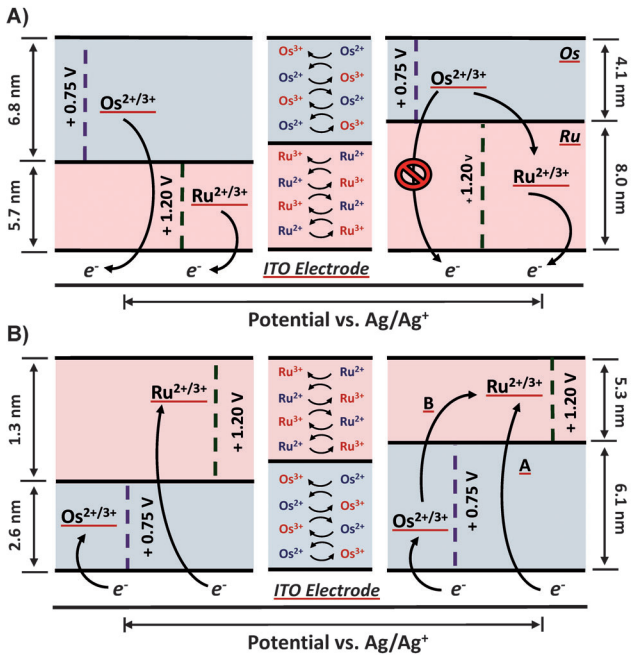

Scheme 2. Electron transfer in self-propagating molecule-based assemblies created by sequence-dependent assembly II and III (Scheme 1). A) Oxidative mechanism of electron transfer observed for SPMAs created by sequence-dependent assembly II. For SPMAs with a Ru surface–interface thickness under 5.7 nm, direct oxidation of the Os and Ru metal centers by the ITO electrode is possible (left). At higher Ru surface–interface thicknesses over 8.0 nm, the oxidation the Os^{2+} metal centers is catalytically mediated by the Ru^{3+} metal centers (right). B) Reductive mechanism of electron transfer observed for SPMAs created by sequence-dependent assembly III. For SPMAs with an Os surface–interface thickness under 2.6 nm, direct reduction of the Os and Ru metal centers by the ITO electrode occurs (left). At intermediate Os surface–interface thicknesses 3.8–6.1 nm, two distinct reduction pathways are observed. Pathway A: direct electron transfer from the ITO electrode to the Ru^{3+} centers, and Pathway B: catalytically mediated electron transfer by the Os^{2+} metal centers (right). At higher thicknesses (over 6.1 nm) complete isolation of the metal centers is observed (not shown).

Moreover, in the negative scan direction, reduction of the Os layer from $Os^{3+}\rightarrow Os^{2+}$ is absent. At the half-wave potential of the $Os^{2+/3+}$ redox couple, all the Ru^{3+} centers have been reduced, and there is no pathway available to reduce the Os^{3+} in the outer layer, and consequently charge trapping occurs. This charge trapping is further manifested by a decrease in the intensity of the oxidative pre-wave in the 2nd scan-cycle (Figure S6). This decrease in intensity is attributed to a decrease in the available Os^{2+} metal centers in the 2nd scan cycle. Overall, the electron transport is mediated only by the $Ru^{2+/3+}$ redox couple and occurs unidirectional towards the ITO electrode, and SPMA II | Ru_3-Os_1 acts as a molecular rectifier.[11] Interestingly, below a certain threshold thickness (8.0 nm) of the ruthenium layer, the electrochemical behavior of self-propagating molecule-based assemblies created by sequence-dependent assembly II is completely reversible (Figure 2 A and S7). An intriguing question that arises is: would similar results be obtained if the successive arrangement of molecular components **1** and **2** is reversed, that is, deposition of complex **2** is followed by complex **1**. To address this question, several self-propagating molecule-based assemblies were prepared by sequence-dependent assembly III.

In sequence-dependent assembly III, two electron-transfer pathways (A and B) were observed depending on the surface–interface thickness of the osmium layer and the scan rate of the electrochemical experiments (Scheme 2 B). For self-propagating molecule-based assemblies with a relatively small surface–interface thickness (2.6 nm; SPMA III | Os_1-Ru_1), reversible behavior of both redox couples **1** and **2** is observed at scan rates of 100, 400, and 700 $mV\,s^{-1}$, respectively (Figure 3 A). The reversible electron transfer occurs by pathway A (Scheme 2 B), and is mediated by the porosity of our assemblies.[3c,12] Upon increasing the thickness to 3.8 nm (SPMA III | Os_2-Ru_2), reversible behavior is observed at

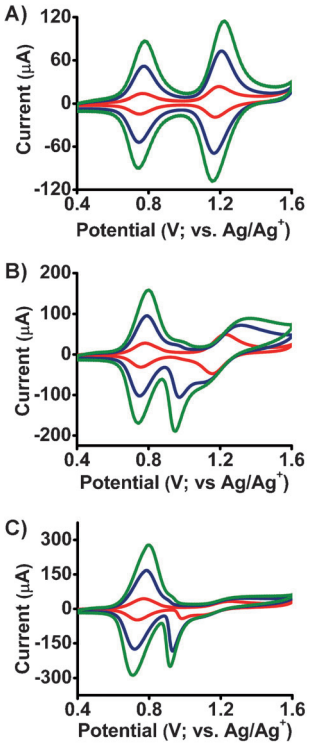

Figure 3. CVs of self-propagating molecule-based assemblies (SPMAs) constructed by sequence-dependent assembly (III; Scheme 1). A) CV of SPMA III | Os_1-Ru_1 on ITO, with an Os thickness of 2.6 nm and a Ru thickness of 1.3 nm, at a scan rate of 100 $mV\,s^{-1}$ (red trace), 400 $mV\,s^{-1}$ (blue trace), and 700 $mV\,s^{-1}$ (green trace). B) CV of SPMA III | Os_2-Ru_2 on ITO, with an Os thickness of 3.8 nm and a Ru thickness of 5.0 nm, at a scan rate of 100 $mV\,s^{-1}$ (red trace), 400 $mV\,s^{-1}$ (blue trace) and 700 $mV\,s^{-1}$ (green trace), demonstrating the evolution of a reductive catalytic pre-wave at approximately 1.00 V. C) CV of SPMA III | Os_3-Ru_2 on ITO, with an Os thickness of 6.1 nm and a Ru thickness of 5.3 nm, at a scan rate of a 100 $mV\,s^{-1}$ (red trace), 400 $mV\,s^{-1}$ (blue trace), and 700 $mV\,s^{-1}$ (green trace), demonstrating the permanent presence and evolution of a reductive catalytic pre-wave at ≈1.00 V.

a scan rate of 100 mV s^{-1} (Figure 3B; red trace), with a peak-to-peak separation of 71 mV for the $Ru^{2+/3+}$ redox-couple. However, a new reduction wave evolves at about 1.00 V, when the scan rate is increased to 400 mV s^{-1} and 700 mV s^{-1} (Figure 3B; blue and green traces, respectively). This new reduction wave is accompanied by a concurrent increase in the peak-to-peak separation from 71 mV to 254 mV of the $Ru^{2+/3+}$ redox couple. The $Os^{2+/3+}$ redox-couple, in contrast, only exhibits a relatively small change at higher scan rates (24 to 61 mV). The unusually large increase in peak-to-peak separation for the $Ru^{2+/3+}$ redox couple in SPMA III | Os_2-Ru_2 is due to interference from the Os layer, in which the electron transfer at the Os^{3+}/Ru^{2+} interface is thermodynamically unfavorable,[13] and hence becomes more difficult. Oxidation of the Ru^{2+} metal centers still occurs mainly by the large (0.4 V) over-potential that is applied, although the electron transfer through defects and pinholes cannot be excluded.[3c,12] The thermodynamic and kinetic effects of electron transfer at the Os/Ru interface is even more pronounced when the self-propagating molecule-based assembly is reduced. Scanning in the negative direction, two distinct pathways (A and B) were observed, in which the electrode is able to reduce the outer Ru^{3+} centers (Scheme 2B). For Pathway A, at low scan rates (< 100 mV s^{-1}) the electron transfer occurs similarly to the transfer that results in the oxidation, and is mediated by the porosity of our assemblies.[3c,12] When the scan rate is increased a second pathway (B) is preferred.[13] A typical characteristic of Pathway B is that the onset of the reduction from $Os^{3+}\rightarrow Os^{2+}$ forms a conductive path to catalytically reduce the remaining $Ru^{3+}\rightarrow Ru^{2+}$; that is, the Ru^{3+} that has not yet been reduced by means of Pathway A. Since the reduction by Pathway A occurs at 1.20 V and the reduction by means of Pathway B is at 1.00 V, there is a temporary charge trapping between 1.00 and 1.20 V.[13] The increased dominance of the catalytic reduction wave is further exemplified by increasing the Os thickness to 6.1 nm (SPMA III | Os_3-Ru_2). Even at 100 mV s^{-1} a predominant catalytic reduction peak is observed at about 1.00 V, although the original reduction is still observable (Figure 3C; red trace). Further increasing the scan rate to 700 mV s^{-1} decreases the original oxidation/reduction wave almost completely and only the catalytic reduction peak remains (Figure 1C and Figure 3C). Moreover, the anodic peak potential (E_{pa}) for the ruthenium reduction shifts by 80 mV, from 0.990 V to 0.910 V, owing to the more catalytic character of the electron transfer to the ITO electrode. The shift to a more catalytic nature of the ruthenium reduction—upon increasing the osmium surface–interface thickness—is also evident from the current responses of SPMA III | Os_1-$Ru_1\rightarrow$SPMA III | Os_4-Ru_1 after applying a potential step from 1.60–1.00 V (Figure S8). However, when the Os thickness is further increased to 11 nm (SPMA III | Os_4-Ru_4), the oxidation/reduction processes associated with the $Ru^{2+/3+}$ redox couple is absent in the CV (Figure S9). At this Os thickness, the ruthenium centers are completely isolated from the surface. The mechanism underlying electron transfer in self-propagating molecule-based assemblies, prepared by sequence-dependent assembly III, with an Os thickness up to 6.1 nm is graphically illustrated in Scheme 2B.

In sequence-dependent assembly IV, the multi-component self-propagating molecule-based assemblies were obtained by deposition from a solution containing an equimolar amount of complexes **1** and **2** (Scheme 1). These self-propagating molecule-based assemblies exhibit reversible behavior for redox couples $Os^{2+/3+}$ and $Ru^{2+/3+}$ up to a thickness of 30.0 nm (Figure S10). For instance, a 12.5 nm-thick self-propagating molecule-based assembly (SPMA IV | $(Os\text{-}Ru)_5$) displays reversible behavior between 25 and 700 mV s^{-1} (Figure 1D and Figure 4A). The electrochemical

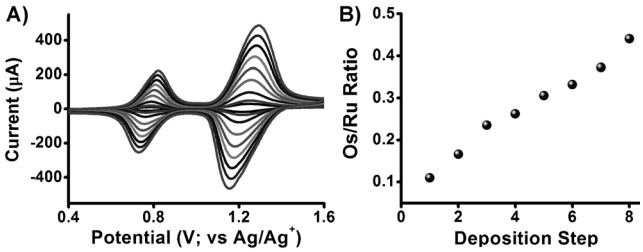

Figure 4. CVs of self-propagating molecular-based assemblies constructed by sequence-dependent assembly (IV; Figure 1). A) CVs of SPMA IV | $(Os\text{-}Ru)_5$ on ITO at scan rates between 25 and 700 mV s^{-1}, with a thickness of 12.5 nm demonstrating the reversible and surface-confined oxidation/reduction of the $Os^{2+/3+}$ and $Ru^{2+/3+}$ redox-couples. B) Increase in the Os/Ru ratio, as determined by the charges in the CVs of the corresponding redox couples, upon increasing the number of deposition steps; SPMA IV | $(Os\text{-}Ru)_{1\rightarrow 8}$.

behavior reflects the electrochemical characteristics obtained upon repeatedly alternating the assembly sequence of the molecular components (sequence-dependent assembly I). Interestingly, using this assembly sequence, a change in the Os and Ru ratio is observed when moving from SPMA IV | $(Os\text{-}Ru)_1\rightarrow$SPMA IV | $(Os\text{-}Ru)_8$. For very thin films (2.8 nm; SPMA IV | $(Os\text{-}Ru)_1$) the Os/Ru ratio is about 1:10, which increases to approximately 1:2 upon increasing the self-propagating molecule-based assembly thickness to 29.8 nm (SPMA IV | $(Os\text{-}Ru)_8$; Figure 4B and S11).

Our results clearly demonstrate the importance of the assembly sequence and the surface–interface thickness of the molecular components **1** and **2** on the physicochemical properties, which are important for device fabrication. For instance self-propagating molecule-based assemblies suitable for ternary memory devices in high-density data storage (HDDS) can be constructed by sequence-dependent assembly I.[8a,14] This sequence-dependent assembly allows the independent addressing of each type of metal-center that displays reversible, reliable, and stable electrochemical properties. The individual addressability of both molecular components in SPMA I may also be ideal for applications in three-dimensional integrated circuits (3D-ICs). Other sequence-dependent assembly strategies result in the formation of molecular rectifiers, among others. The observed unidirectional current flow, and the diverse electrochemical properties (sequence-dependent assembly II and III) are of particular interest for fabricating solar-cells, where charge trapping and unidirectional current flows are important.[15] Along with the photo-activity of Ru-polypyridyl complexes in

solar cells,[16] it is important to consider how to assemble those complexes in binary systems, for example, blended or separated.[17]

The electrochemical rectification of redox-active polymers in a bilayer fashion has been known since the seminal work of Murray and Wrighton.[11,13,18] Unidirectional current flows have been subsequently reported between redox-active organic (mono/multi)-layers and ferrocyanide solutions,[19] or in redox active (ionic) polymers that might contain metal complexes.[20] However, the versatility of the sequence-dependent assembly and the resulting properties of the demonstrated interfaces are unprecedented. These films not only exhibit different electrochemical behavior upon changing the assembly sequence, they also dramatically change their behavior as a function of a controllable surface–interface thickness. This thickness in turn controls the electron transfer at the metal/metal interface. Together they determine the overall material properties in each sequence-dependent assembly.

In conclusion, four different types of interfaces were demonstrated with two molecular components, **1** and **2**. As a result of the applied sequence-dependent assembly, different electrochemical behavior was observed for all four self-propagating molecule-based assemblies. Successive deposition of the molecular components resulted in the occurrence of catalytic pre-waves that oxidized/reduced the outer layer of the self-propagating molecule-based assembly, depending on which component was deposited first. If ruthenium was deposited first (SPMA II | Ru_x-Os_y), catalytic oxidation of the outer Os layer was observed, provided that the thickness of the Ru layer exceeded 8.0 nm. However, instead of this thermodynamic effect, a kinetic effect was observed when the osmium was deposited first (SPMA III | Os_x-Ru_y). The two observed Pathways A and B for electron transfer to the outer Ru layer were strongly dependent on the scan rate and the thickness of the Os layer. Assembling the molecular components in an alternating fashion (SPMA I | Ru_x-Os_y), or from a mixture of **1** and **2** (SPMA IV | Ru-Os)$_{x+y}$), however, resulted in a reversible oxidation/reduction process of both metal centers independent of the self-propagating molecule-based assembly thickness. Our work unequivocally demonstrates that upon changing the sequence-dependent assembly strategy and assembly thickness, the electrochemical properties of self-propagating molecule-based assemblies can be controlled. To this end, the sequence-dependent assembly concept is unlikely to be limited only to interfaces; it might also be applied in multi-component systems in solution, including self-sorting assemblies and molecular networking.[6]

Received: September 15, 2012
Published online: November 20, 2012

Keywords: electrochemistry · interfaces · metal complexes · molecular materials · sequence-dependent assembly

[1] a) D. Frattarelli, M. Schiavo, A. Facchetti, M. A. Ratner, T. J. Marks, *J. Am. Chem. Soc.* **2009**, *131*, 12595; b) A. N. Rashid, C. Erny, P. Gunter, *Adv. Mater.* **2003**, *15*, 2024.

[2] a) R. P. Ortiz, A. Facchetti, T. J. Marks, *Chem. Rev.* **2010**, *110*, 205; b) H. Klauk, U. Zschieschang, J. Pflaum, M. Halik, *Nature* **2007**, *445*, 745.

[3] a) K. I. Terada, H. Nakamura, K. Kanaizuka, M. A. Haga, Y. Asai, T. Ishida, *ACS Nano* **2012**, *6*, 1988; b) G. Sedghi, V. M. Garcia-Suarez, L. J. Esdaile, H. L. Anderson, C. J. Lambert, S. Martin, D. Bethell, S. J. Higgins, M. Elliott, N. Bennett, J. E. Macdonald, R. J. Nichols, *Nat. Nanotechnol.* **2011**, *6*, 517; c) L. Motiei, M. Lahav, A. Gulino, M. Iron, M. E. van der Boom, *J. Phys. Chem. B* **2010**, *114*, 14283; d) T. Kurita, Y. Nishimori, F. Toshimitsu, S. Muratsugu, S. Kume, H. Nishihara, *J. Am. Chem. Soc.* **2010**, *132*, 4524; e) N. Tuccitto, V. Ferri, M. Cavazzini, S. Quici, G. Zhavnerko, A. Licciardello, M. A. Rampi, *Nat. Mater.* **2009**, *8*, 41; f) G. Sedghi, K. Sawada, L. J. Esdaile, M. Hoffmann, H. L. Anderson, D. Bethell, W. Haiss, S. J. Higgins, R. J. Nichols, *J. Am. Chem. Soc.* **2008**, *130*, 8582.

[4] a) K. Ariga, Q. Ji, J. P. Hill, Y. Bando, M. Aono, *NPG Asia Mater.* **2012**, *4*, e17; b) R. Makiura, S. Motoyama, Y. Umemura, H. Yamanaka, O. Sakata, H. Kitagawa, *Nat. Mater.* **2010**, *9*, 565; c) O. Shekhah, H. Wang, M. Paradinas, C. Ocal, B. Schüpbach, A. Terfort, D. Zacher, R. A. Fischer, C. Wöll, *Nat. Mater.* **2009**, *8*, 481; d) K. Kanaizuka, R. Haruki, O. Sakata, M. Yoshimoto, M. Akita, H. Kitagawa, *J. Am. Chem. Soc.* **2008**, *130*, 15778.

[5] The naming of the four self-propagating molecule-based assemblies (I–IV) in consecutive order is as follows: SPMA I | Ru_x-Os_y; SPMA II | Ru_x-Os_y; SPMA III | Os_y-Ru_x; and SPMA IV | (Ru-Os)$_{x+y}$, where x and y denote the number of deposition steps in which complex **1** and **2** was deposited (Scheme 1).

[6] a) V. E. Campbell, X. de Hatten, N. Delsuc, B. Kauffmann, I. Huc, J. R. Nitschke, *Nat. Chem.* **2010**, *2*, 684; b) H. Deng, C. J. Doonan, H. Furukawa, R. B. Ferreira, J. Towne, C. B. Knobler, B. Wang, O. M. Yaghi, *Science* **2010**, *327*, 846; c) B. H. Northrop, Y.-R. Zheng, K.-W. Chi, P. J. Stang, *Acc. Chem. Res.* **2009**, *42*, 1554; d) R. Sknepnek, J. A. Anderson, M. H. Lamm, J. Schamlian, A. Travesset, *ACS Nano* **2008**, *2*, 1259; e) J. M. Lehn, *Science* **2002**, *295*, 2400.

[7] a) L. Motiei, M. Feller, G. Evmenenko, P. Dutta, M. E. van der Boom, *Chem. Sci.* **2012**, *3*, 66, and references therein.

[8] a) G. de Ruiter, L. Motiei, J. Choudhury, N. Oded, M. E. van der Boom, *Angew. Chem.* **2010**, *122*, 4890; *Angew. Chem. Int. Ed.* **2010**, *49*, 4780; b) L. Motiei, Y. Yao, J. Choudhury, H. Yan, T. J. Marks, M. E. van der Boom, A. Facchetti, *J. Am. Chem. Soc.* **2010**, *132*, 12528; c) L. Motiei, M. Lahav, D. Freeman, M. E. van der Boom, *J. Am. Chem. Soc.* **2009**, *131*, 3468.

[9] L. Motiei, M. Altman, T. Gupta, F. Lupo, A. Gulino, G. Evmenenko, P. Dutta, M. E. van der Boom, *J. Am. Chem. Soc.* **2008**, *130*, 8913.

[10] R. Kaminker, L. Motiei, A. Gulino, I. Fragalà, L. J. W. Shimon, G. Evmenenko, P. Dutta, M. A. Iron, M. E. van der Boom, *J. Am. Chem. Soc.* **2010**, *132*, 14554.

[11] a) H. D. Abruna, P. Denisevich, M. Umana, T. J. Meyer, R. W. Murray, *J. Am. Chem. Soc.* **1981**, *103*, 1–5; b) P. Denisevich, K. W. Willman, R. W. Murray, *J. Am. Chem. Soc.* **1981**, *103*, 4727.

[12] L. Motiei, R. Kaminker, M. Sassi, M. E. van der Boom, *J. Am. Chem. Soc.* **2011**, *133*, 14264.

[13] C. R. Leidner, R. W. Murray, *J. Am. Chem. Soc.* **1985**, *107*, 551.

[14] G. de Ruiter, Y. H. Wijsboom, N. Oded, M. E. van der Boom, *ACS Appl. Mater. Interfaces* **2010**, *2*, 3578–3585.

[15] P. Wurfel, *Physics of Solar Cells: From Basic Principles to Advanced Concepts*, 2nd ed., Wiley-VCH, Weinheim, **2009**.

[16] A. Reynal, E. Palomares, *Chem. Eur. J.* **2011**, *17*, 4509.

[17] M. D. McGehee, M. A. Topinka, *Nat. Mater.* **2006**, *5*, 675.

[18] a) C. E. D. Chidsey, R. W. Murray, *Science* **1986**, *231*, 25; b) D. K. Smith, G. A. Lane, S. M. Wrighton, *J. Am. Chem. Soc.* **1986**, *108*, 3522.

[19] a) S. Berchmans, C. Ramalechume, V. Lakshmi, V. Yegnaraman, *J. Mater. Chem.* **2002**, *12*, 2538; b) S. K. Oh, L. A. Baker, R. M. Crooks, *Langmuir* **2002**, *18*, 6981.
[20] a) R. J. Alvarado, J. Mukherjee, E. J. Pacsial, D. Alexander, F. M. Raymo, *J. Phys. Chem. B* **2005**, *109*, 6164; b) J. Hjelm, R. W. Handel, A. Hagfeldt, E. C. Constable, C. E. Housecroft, R. J. Forster, *Inorg. Chem.* **2005**, *44*, 1073; c) D. M. DeLongchamp, M. Kastantin, P. T. Hammond, *Chem. Mater.* **2003**, *15*, 1575; d) C. G. Cameron, P. G. Pickup, *J. Am. Chem. Soc.* **1999**, *121*, 11773; e) K. Araki, L. Angnes, H. E. Toma, *Adv. Mater.* **1995**, *7*, 554.

